Full $0\hbar\omega$ shell model calculation of the binding energies of the $1f_{7/2}$ nuclei

E. Caurier,[1] G. Martínez-Pinedo,[2,3] F. Nowacki,[4] A. Poves,[5] J. Retamosa,[6] and A. P. Zuker[1]
[1]*Institut de Recherches Subatomiques (IN2P3-CNRS-Université Louis Pasteur) Bâtiment 27/1, F-67037 Strasbourg Cedex 2, France*
[2]*W. K. Kellogg Radiation Laboratory, California Institute of Technology, Pasadena, California 91125*
[3]*Institute of Physics and Astronomy, University of Århus, DK-8000 Århus, Denmark*
[4]*Laboratoire de Physique Théorique de Strasbourg, 3-5 rue de L'Université, F-67084 Strasbourg Cedex, France*
[5]*Departamento de Física Teórica C-XI, Universidad Autónoma de Madrid, E-28049 Madrid, Spain*
[6]*Departamento de Física Atómica y Nuclear, Universidad Complutense de Madrid, E-28040 Madrid, Spain*
(Received 22 September 1998)

Binding energies and other global properties of nuclei in the middle of the pf shell, such as $M1$, $E2$, and Gamow-Teller sum rules, have been obtained using a new shell model code (NATHAN) written in quasispin formalism and using a j-j-coupled basis. An extensive comparison is made with the recently available shell model Monte Carlo results using the effective interaction KB3. The binding energies for nearly all the $1f_{7/2}$ nuclei are compared with the measured (and extrapolated) results. [S0556-2813(99)05303-0]

PACS number(s): 21.10.Dr, 21.60.Cs, 27.40.+z

I. INTRODUCTION

Detailed shell model calculations in the full pf-shell have been recently carried out [1–3] up to $A=52$ using a realistic G-matrix [4] with the monopole modifications of Ref. [5] (KB3). These calculations could only be done due to the availability of the m-scheme code ANTOINE [6]. It has allowed us to tackle the largest dimensionalities ever reached by any exact diagonalization shell model code [7]. The main disadvantage of ANTOINE is that J and T are not good quantum numbers and the dimensions of the matrices are maximal.

One is then led to develop new tools to deal with the increasingly large model spaces needed in shell-model calculations. In this paper we present the first results obtained using a new code [NATHAN] [8,9] that works in the j-j coupling scheme and uses the quasispin formalism. This code retains the main idea of the code ANTOINE to calculate efficiently all nonzero matrix elements during the diagonalization procedure. It can be used either for unrestricted calculations as is the case here, or for nuclei in which seniority truncations are physically sound as in the Sn region. The use of a j-j coupling scheme allows us to reduce the memory requirements with the penalty of an increase in CPU time. This increase is not so important as new computers double their speed every year and new shared-memory parallel machines are now available that allow for a relatively easy parallelization.

This paper has several goals: (a) to report on results of the very large shell model calculations that can now be performed; (b) to use them as benchmarks for the new approximate methods of solving the large scale shell model problem, e.g., Monte Carlo shell model [10] or quantum Monte Carlo diagonalization method [11]; (c) to analyze the systematics of binding energies for nuclei $40\leqslant A\leqslant 56$, $20\leqslant N$, $Z\leqslant 28$, extending the already published results for $A=47$, 48 and 49 down to the beginning of the shell and up to the $N=Z=28$ closure, studying the effect of the scaling with the mass of the matrix elements. These three objectives will be dealt with in Secs. II, III, and IV.

II. THE SHELL MODEL CODE "NATHAN"

For a long time, shell model calculations have been limited to light nuclei or to heavier ones with only a few particles outside closed shells. Besides the well-known problems related to the determination of a good effective interaction for large valence spaces, there are compelling technical limitations due to the explosive increase of the dimensions of the matrices to diagonalize. The diagonalization in itself is not a problem since, in general, only a few eigenvectors are needed and in this case the Lanczos method is very efficient. For very large matrices, the convergence of the method is optimized by preliminary calculations in a truncated space. The fundamental problem is that we have to deal with "giant" matrices, giant meaning that the number of its nonzero elements is so large that it is impossible to store all of them before doing the Lanczos procedure. For this reason, one needs to compute all the nonzero terms at each new Lanczos iteration. It is clear that modern shell model codes must tackle this problem and that the quality of the code will be directly related to its performance in the calculation of nonzero terms during the Lanczos procedure itself.

The first breakthrough in this direction was due to the Glasgow group [12]. They took advantage of the simplicity of the m-scheme. In their code, each Slater determinant (SD) is represented by an integer word and each individual state by a bit in this word. Bit manipulation and bisection algorithms allow for a fast generation of the matrix elements. The shell model code ANTOINE adds some important improvements to the Glasgow method. Its basic principles are the following:

Each state of the basis is written as the product of two SD's, one for protons and one for neutrons $|I\rangle=|i,\alpha\rangle$, where we use capital letters (I,J) for states in the total space, lower case latin letters (i,j) for proton states, and lower case greek letters (α,β) for neutron states.

Even if the dimensions are very large in the total space, they are much smaller in the proton and in the neutron spaces separately. For example, the 1 963 461 SD's with $M=0$ in

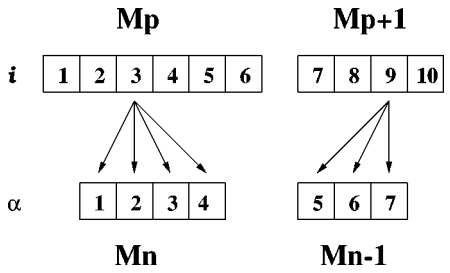

FIG. 1. Illustration of pn factorization.

^{48}Cr are generated from the ^{44}Ca SD's for all possible M values (just 4865).

The i and α SD's can be classified by their J_z values M_p and M_n. The total M being fixed, proton and neutron SD's will be associated only if $M_p+M_n=M$. A graphical illustration is given below.

We can now follow in the graph how the basis is constructed. Let us first make a loop on i, and then on α. Since we have four α states in the first ''block'' (M_p,M_n) the SD $i=1$ generates the states $I=1,2,3,4$, the SD $i=2$ generates the states $I=5,6,7,8$ and so on. When we arrive at the second ''block'' (M_p+1,M_n-1), $6\times4=24I$ states have been built. Now we have three α SD's, meaning that $i=7$ generates $I=25,26,27$. It is clear that for each i state the allowed α states run *without discontinuity* between a minimum and a maximum value; therefore it is possible to construct *numerically* an array $R(i)$ such that

$$I=R(i)+\alpha.$$

In our example we have $1=R(1)+1$, $5=R(2)+1$, $25=R(7)+5,\ldots$; thus, knowing i, α, and $R(i)$ we get immediately I. Afterwards, the program proceeds as follows: for the pp and nn matrix elements all the $[R(i),R(j),W]$ and (α,β,W), where $\langle i|H|j\rangle=W$ and $\langle\alpha|H|\beta\rangle=W$, are precalculated and stored. Therefore, in the Lanczos procedure a simple loop on α and i will generate all the pp and nn matrix elements (I,J,W). For instance, in the ^{48}Cr case, 102 886 (i,j,W) terms generate 46 484 396 (I,J,W).

For the pn matrix elements the situation is only a bit more complicated. Let us assume that the SD's i and j are connected by the one-body operator $a_q^\dagger a_r$ (labeled by p), with $q=nljm$ and $r=n'l'j'm'$ and $m'-m=\Delta m$. We precalculate all the $[R(i),R(j),p]$ and (α,β,μ). Conservation of the total M implies that the proton operators with Δm must be associated with the neutron operators with $-\Delta m$. Thus we could draw a scheme equivalent to the one above for the proton and neutron one-body operators (see Fig. 1). In the same way as we did before for $I=R(i)+\alpha$, we can now define $K=Q(p)+\mu$. The two-body proton-neutron matrix element that connect the states (i,α) and (j,β) will be denoted by $V(K)$.

Once $[R(i),R(j),Q(p)]$ and (α,β,μ) stored, the nonzero elements of the matrix in the full space are generated with three integer additions:

$$I=R(i)+\alpha,$$

$$J=R(j)+\beta,$$

$$K=Q(p)+\mu,$$

$$H_{I,J}=H_{J,I}=V(K).$$

Another improvement that the code ANTOINE incorporates is an initial Lanczos procedure with the operators J^2 and T^2, i.e., a projection onto good J and T. Basis states of good J and T are then used as initial states for the Hamiltonian's Lanczos iterations. This accelerates the convergence dramatically.

The main disadvantage of the m-scheme is that the space contains all the states with $J\geqslant J_z$ and $T\geqslant T_z$. The fundamental limitation is the disk space needed to store the Lanczos vectors. For that reason, we have adapted the idea of separating proton and neutron spaces to a coupled basis. Now, each i and α represents a combination of SD's coupled to good angular momentum with the usual techniques of the Oak-Ridge/Rochester group [13]. The ''blocks'' are labeled by J_p and J_n. But instead of having a one-to-one association $(M_p+M_n=M)$, for a given J_p we now have all the possible J_n

$$J_{\min}\leqslant J_n\leqslant J_{\max}$$

$$\text{with}\ \ J_{\min}=|J_0-J_p|\ \ \text{and}\ \ J_{\max}=J_0+J_p.$$

The continuity between the first state with $J_{\min}$ and the last with $J_{\max}$ is maintained and consequently the fundamental relation $I=R(i)+\alpha$ still holds. The generation of the proton-proton (neutron-neutron) matrix elements proceeds exactly as in m-scheme.

For the proton-neutron matrix elements the one-body operators in each space can be written as $O_p^\lambda=(a_{j_1}^\dagger a_{j_2})^\lambda$. There exists a strict analogy between Δm in m-scheme and λ in the coupled scheme. Hence, we can still establish a relation $K=Q(p)+\omega$. The matrix elements read now:

$$H_{I,J}=H_{J,I}=h_{i,j}^*h_{\alpha,\beta}^*W(K)$$

$$\text{with}\ \ h_{i,j}=\langle i|O_p^\lambda|j\rangle\ \ \text{and}\ \ h_{\alpha,\beta}=\langle\alpha|O_\omega^\lambda|\beta\rangle,$$

$$W(K)\propto V(K)*\begin{Bmatrix} i & \alpha & J\\ j & \beta & J\\ \lambda & \lambda & 0\end{Bmatrix},$$

$V(K)$ being a two-body matrix element.

As in m-scheme we have to perform the three integer additions which generate I, J, and K, but in addition we have two floating point multiplications, since $h_{i,j}$ and $h_{\alpha,\beta}$, which in m-scheme are just a phase, are now a product of cfp's and $9j$ coefficients (see formula 3.10 of Ref. [13]). Therefore, the generation of the proton-neutron matrix elements requires three integer additions, as in the m-scheme code, plus two floating point multiplications.

In summary, the two codes turn out to be complementary. The coupled formalism is more efficient in the following cases.

For $J=0^+$ states (the dimensions are two orders of magnitude smaller than in the m-scheme) and to a lesser extent for low spin states.

TABLE I. m-scheme and $J=0$ dimensions in the full pf shell.

Nucleus	m scheme	$J=0$ dimension
^{48}Ti	634 744	14 177
^{50}Ti	1 967 848	39 899
^{52}Ti	2 843 770	55 944
^{50}Cr	14 625 240	267 054
^{52}Cr	45 734 928	773 549
^{54}Cr	66 262 352	1 093 850
^{52}Fe	109 954 620	1 777 116
^{54}Fe	345 400 174	5 220 621
^{56}Fe	501 113 392	7 413 488
^{56}Ni	1 087 455 228	15 443 684

When many Lanczos iterations are needed (as for the calculation of strength functions).

When seniority truncations are reasonable.

When the size of the m-scheme Lanczos vectors exceeds the storage capacity of the disks.

In other cases, the m-scheme code ANTOINE remains a better option. The two codes run on ordinary workstations. Indeed, the use of parallel computers should improve strongly their performances.

The code NATHAN has made it possible to carry out calculations that, if made in m-scheme, would involve more than one billion $M=0$ Slater determinants, as in our calculation of the ground state of ^{56}Ni in the full pf-shell. The dimensions of the $J=0$ matrices together with their equivalent m-scheme dimensions are listed in Table I for some of the nuclei we have studied in this work. Once the energy and the wave function of the ground state of a given nucleus is obtained, it is easy to build the doorway states (also named sum rule states) acting with the different transition operators Ω^{λ} on it. The norm of the doorway gives the nonenergy weighted sum rule for the operator. If the doorway is used as starting vector in the Lanczos process, successive iterations provide the energy to the nth weighted sum rules or equivalently the different moments of the strength function of the transition operator chosen. Notice that already with two iterations we obtain the norm, the centroid, the width and the skewness of the distribution of strength. These are averaged quantities that can be also accessed by the new stochastic approaches to the shell model problem, as for instance the shell model Monte Carlo (SMMC), and we shall devote the next section to compare the approximate and exact solutions.

III. BENCHMARKS AND COMPARISON WITH SMMC RESULTS

With the advent of the stochastic approximations to the solution of the shell model problem, it becomes crucial to dispose of large enough sets of exacts results in order to benchmark the accuracy of the new methods and to uncover their strong and weak aspects. We have chosen to make this comparison with the set of nuclei studied by Langanke *et al.* [14] using Caltech's SMMC. The effective interaction KB3 is used throughout, with effective charges 1.35 for protons and 0.35 for neutrons, bare g-factors and unquenched Gamow-Teller operator. The choice of an isoscalar effective charge of 1.7 in [14] instead of the canonical value of 2 leads to values that underpredict the experimental quadrupole transition rates. However this is irrelevant for our purpose of comparing SMMC and exact SM diagonalizations. SMMC involves two extrapolations; one in temperature and another in the parameter that has to be introduced [15] in order to change the sign of those terms of the Hamiltonian that have ''bad'' sign and that, if taken at their original value, will spoil the convergence of the Monte Carlo method. Both extrapolations will contribute to the final differences with the exact results. While the defaults associated with the impossibility of doing a zero temperature calculation are smooth and predictable, those associated with the change of sign of the ''bad''-sign terms are less well under control.

TABLE II. Valence space energies (in MeV) and $B(E2)$ sum rules (in e^2 fm^4), exact diagonalization vs shell model Monte Carlo results. The SMMC results have been obtained at finite temperature and include an internal excitation energy of 0.5 MeV. The typical error bar of the SMMC energies is 0.4 MeV.

Nucleus	E(SM) (shell model)	E(SM) (SMMC)	$\Sigma B(E2)$ (shell model)	$\Sigma B(E2)$ (SMMC)
^{48}Ti	-24.6	-23.9	476	455 ± 25
^{50}Ti	-27.7	-27.2	405	465 ± 50
^{52}Ti	-25.4	-24.9	477	465 ± 55
^{54}Ti	-22.0	-21.4	445	450 ± 80
^{48}Cr	-32.9	-32.3	978	945 ± 45
^{50}Cr	-40.5	-40.0	913	890 ± 90
^{52}Cr	-46.0	-45.6	690	645 ± 75
^{54}Cr	-47.0	-46.3	888	890 ± 90
^{56}Cr	-45.5	-44.8	825	840 ± 90
^{52}Fe	-54.3	-53.7	1016	1055 ± 50
^{54}Fe	-62.8	-62.7	764	750 ± 80
^{56}Fe	-66.4	-65.8	1019	990 ± 6
^{58}Fe	-67.7	-66.7	1117	1010 ± 65
^{60}Fe	-67.0	-65.8	1052	1105 ± 65
^{56}Ni	-78.5	-77.8	572	515 ± 65
^{62}Ni	-89.5	-87.6	823	1010 ± 25
^{64}Ni	-89.9	-87.7	773	1165 ± 80
^{64}Zn	-106.3	-104.8	1157	1225 ± 65

In Table II we gather the energies and the E_2 sum rules $[\Sigma_i B(E2)\ \ 0^+\rightarrow 2_i^+]$. SMMC gives energies that are above the exact values by about 0.5 MeV in most of the cases. This is consistent with a residual ''heating'' in SMMC. However, for the heaviest part of the set of nuclei studied, the discrepancies grow up to reach 2 MeV, indicating problems in the extrapolation linked to the ''bad''-sign terms. The E_2 sum rules are nicely reproduced by SMMC except in a couple of cases, ^{62}Ni and^{64}Ni where the exact results are clearly missed.

In Table III the comparison is extended to M_1 and Gamow-Teller sum rules. In most cases, the 10–15% error bars of the SMMC numbers suffice to embrace the exact result. Nevertheless, there still remain some large deviations in the Gamow-Teller strength of ^{60}Fe, ^{62}Ni, ^{64}Ni, and ^{64}Zn.

The outcome of this comparison is two-sided. On the one side, it validates SMMC at the 0.5–1.0 MeV level for the ground state energies and at the 20% level for the sum rules. On the other side, there are cases in which the discrepacies

TABLE III. $M1$ (in μ_N) and Gamow-Teller sum rules, exact diagonalization vs shell model Monte Carlo results.

Nucleus	$\Sigma B(M1)$ (shell model)	$\Sigma B(M1)$ (SMMC)	$\Sigma B(GT_+)$ (shell model)	$\Sigma B(GT_+)$ (SMMC)
^{48}Ti	10.6	10.2±1.2	1.26	1.13±0.18
^{50}Ti	12.6	12.5±1.0	1.24	1.47±0.16
^{52}Ti	12.9	12.5±1.0	0.99	1.11±0.16
^{54}Ti	13.4	13.5±1.5	0.89	0.97±0.21
^{48}Cr	12.0	13.8±1.7	4.13	4.37±0.35
^{50}Cr	13.9	14.5±2.5	3.57	3.51±0.27
^{52}Cr	15.6	18.9±2.2	3.33	3.51±0.19
^{54}Cr	16.5	13.0±2.5	2.24	2.21±0.22
^{56}Cr	16.3	16.2±2.0	1.92	1.50±0.21
^{52}Fe	17.2	18.9±1.4	6.92	7.10±0.42
^{54}Fe	18.9	16.5±2.8	6.33	6.05±0.45
^{56}Fe	19.4	20.4±3.0	4.69	3.99±0.27
^{58}Fe	18.8	20.3±3.0	3.12	3.06±0.28
^{60}Fe	18.2	17.3±2.1	2.60	1.80±0.24
^{56}Ni	22.8	23.0±1.2	10.2	9.86±0.38
^{62}Ni	20.7	19.6±2.9	4.38	3.43±0.40
^{64}Ni	19.3	18.9±2.7	3.44	1.73±0.29
^{64}Zn	21.6	23.6±2.2	5.54	4.13±0.34

grow larger without an evident cause. This could represent a serious threat to the predictive power of SMMC, although it is possible that a more thorough control of the different extrapolations could bring these isolated cases into line with the overall results.

IV. BINDING ENERGIES

The code NATHAN has given us the opportunity to complete our stock of binding energies of pf-shell nuclei, in the full space, using the effective interaction KB3. It is our aim now to verify that we can describe the ground state energies at the same level of accuracy that we have achieved for the excitation energies (~200 keV). A remark is timely here: the monopole part of the interaction KB3 was fixed by $1f7/2$ nuclei, when only extremely truncated calculations were feasible. Therefore its non-$1f7/2$ monopoles are not well determined. Furthermore, its quasiparticle gap around ^{56}Ni is too strong by about 1 MeV, which results in a relative underbinding of the nuclei with N or Z larger than 28. For this reason we shall only deal with $1f7/2$ nuclei in this section.

What the shell model calculation produces, $E(\mathrm{SM})$ in the second column of Table IV, is the contribution to the nuclear binding energy of the interaction of the valence particles among themselves. It does not include the Coulomb repulsion among the protons, nor the binding energy of the core (^{40}Ca in our case), nor the interaction among the core and the valence particles. Therefore, in order to compare with the experimental binding energies relative to ^{40}Ca, B_e, we have take into account these quantities.

The Coulomb energies relative to ^{40}Ca can be approximated by the following formula valid for a major shell (π=valence protons, ν=valence neutrons):

$$E_C = e_\pi \pi + V_{\pi\pi}\frac{\pi(\pi-1)}{2} + V_{\pi\nu}\pi\nu. \tag{1}$$

In our previous works [1,3] the values of the constants e_π, $V_{\pi\pi}$, and $V_{\pi\pi}$ were determined from the differences in binding energies between ^{41}Sc and ^{40}Ca(e_π) and the $A=42$ isobars ($V_{\pi\pi}$ and $V_{\pi\nu}$). In this paper we are interested in larger mass region, hence the need of a better determination of the constants in expression (1). In order to do so we have fitted the Coulomb displacement energies of analog states for nuclei between $A=42$ and $A=64$ [16,17]. The resulting parameters are

$$\begin{aligned} e_\pi &= 7.44 \pm 0.02, \\ V_{\pi\pi} &= 0.274 \pm 0.003, \\ V_{\pi\nu} &= -0.049 \pm 0.003. \end{aligned} \tag{2}$$

Another option is to rely in global expressions that are used for the Coulomb term of the mass formulas. We have chosen the one used in Ref. [18]:

$$E_C = 0.700[Z(Z-1) - 0.76(Z(Z-1))^{2/3}]/R_C,$$

$$R_C = e^{1.5/A}A^{1/3}\left(0.946 - 0.573\left(\frac{2T}{A}\right)^2\right). \tag{3}$$

The valence space Coulomb energies obtained from Eq. (3) are very close to those obtained from the fit (2), with discrepancies that never reach 1%. In what follows we shall use the Coulomb energies from the global formula (3).

Besides, one should add the nuclear interaction between a particle in the valence space and the core. The value of this, one body, matrix element is usually taken from the binding energy difference between ^{41}Ca and ^{40}Ca. However we shall proceed otherwise; the effective interaction we have been using (KB3) has been only tested against spectroscopic observables that will not vary if we add to the Hamiltonian terms that only depend on scalars made with the *total* number of valence particles (n) or the *total* isospin (T). Thus, we have the freedom to add the following monopole expression to our Hamiltonian:

$$E_M = e_v n + a\frac{1}{2}n(n-1) + b\left(T(T+1) - \frac{3}{4}n\right), \tag{4}$$

where e_v is an average particle core interaction (hopefully close to the one experimentally determined in $A=41$) and a and b are the isoscalar and isovector global monopole corrections to KB3 that we will fix by a fit to the experimental binding energies relative to ^{40}Ca using the formula:

$$E_B = -B_e = E(SM) + E_C + E_M. \tag{5}$$

The data set is listed in the fourth column of Table IV (the numbers with a star are extrapolated values from [19] not included in the fit) and contains 51 entries. The values of the parameters resulting from the fit are

TABLE IV. Shell model binding energies relative to ^{40}Ca (in MeV), compared with the experimental values (the numbers with a star are extrapolated values from [19] not included in the fit). KB3 interaction without mass dependence (see text for more details).

Nucleus	E(SM)	B_e(Theor.)	B_e(Expt.)	Δ
^{42}Ca	−2.71	19.93	19.84	0.08
^{42}Sc$^{T=1}$	−2.71	12.44	12.64	−0.20
^{42}Sc$^{T=0}$	−2.35	12.20	12.02	0.17
^{42}Ti	−2.71	4.55	4.85	−0.30
^{43}Ca	−2.55	28.19	27.78	0.41
^{43}Sc	−6.67	25.06	24.77	0.29
^{43}Ti	−6.67	17.24	17.12	0.12
^{43}V	−2.55	4.72	5.05*	−0.32
^{44}Ca	−4.99	38.93	38.91	0.02
^{44}Sc	−8.26	35.07	34.47	0.60
^{44}Ti	−13.88	33.06	33.42	−0.37
^{44}V	−8.26	19.16	18.94*	0.22
^{44}Cr	−4.99	7.11	7.84*	−0.74
^{45}Ca	−4.61	46.73	46.32	0.41
^{45}Sc	−10.95	46.06	45.80	0.27
^{45}Ti	−15.49	43.09	42.95	0.14
^{45}V	−15.49	35.00	35.04	−0.04
^{45}Cr	−10.95	21.80	21.79*	0.00
^{45}Mn	−4.61	6.28	6.71*	−0.43
^{46}Ca	−6.73	56.90	56.72	0.18
^{46}Sc	−11.67	54.94	54.56	0.39
^{46}Ti	−20.14	56.02	56.14	−0.12
^{46}V$^{T=1}$	−20.14	47.99	48.31	−0.32
^{46}V$^{T=0}$	−19.77	47.75	47.51	0.24
^{46}Cr	−20.14	39.58	39.92	−0.35
^{46}Mn	−11.67	22.06	22.04*	0.02
^{46}Fe	−6.73	7.57	8.13*	−0.56
^{47}Ca	−6.10	64.20	63.99	0.21
^{47}Sc	−14.05	65.37	65.20	0.17
^{47}Ti	−21.06	65.11	65.02	0.09
^{47}V	−25.07	61.33	61.31	0.02
^{47}Cr	−25.07	52.98	53.08	−0.10
^{47}Mn	−21.06	40.05	40.00*	0.05
^{47}Fe	−14.05	23.61	23.58*	0.03
^{48}Ca	−7.88	73.79	73.94	−0.15
^{48}Sc	−14.13	73.37	73.43	−0.07
^{48}Ti	−24.57	76.65	76.65	0.00
^{48}V	−27.58	71.99	71.85	0.14
^{48}Cr	−32.95	69.20	69.41	−0.21
^{48}Mn	−27.58	55.03	54.81*	0.22
^{48}Fe	−24.57	42.72	43.14*	−0.42
^{48}Co	−14.13	22.48	22.61*	−0.13
^{49}Sc	−16.19	83.23	83.57	−0.34
^{49}Ti	−24.81	84.80	84.79	0.01
^{49}V	−31.01	83.45	83.40	0.04
^{49}Cr	−35.59	79.98	79.99	−0.01
^{49}Mn	−35.59	71.37	71.49	−0.13
^{49}Fe	−31.01	57.61	57.68*	−0.07
^{49}Co	−24.81	41.74	41.90*	−0.15
^{50}Ti	−27.72	95.49	95.73	−0.24
^{50}V	−32.16	92.50	92.74	−0.24
^{50}Cr	−40.54	92.95	92.99	−0.05
^{50}Mn$^{T=1}$	−40.54	84.39	84.58	−0.18
^{50}Mn$^{T=0}$	−40.28	84.26	84.35	−0.09
^{50}Fe	−40.54	75.47	75.64	−0.18
^{50}Co	−32.16	57.55	57.59*	−0.04
^{50}Ni	−27.72	43.06	43.40*	−0.34
^{51}V	−35.31	103.42	103.79	−0.37
^{51}Cr	−41.81	102.10	102.25	−0.15
^{51}Mn	−46.17	98.16	98.26	−0.11
^{51}Fe	−46.17	89.29	89.46	−0.17
^{51}Co	−41.81	75.51	75.74*	−0.23
^{51}Ni	−35.31	59.09	59.12*	−0.03
^{52}Cr	−45.99	114.05	114.29	−0.24
^{52}Fe	−54.27	105.46	105.64	−0.19
^{52}Ni	−45.99	78.08	78.41*	−0.32
^{54}Fe	−62.85	129.63	129.71	−0.07
^{54}Co	−62.85	120.57	120.68	−0.11
^{54}Ni	−62.85	111.15	111.10	0.05
^{56}Ni	−78.46	142.44	141.94	0.50

$$e_v = -8.67 \pm 0.01 \ \text{MeV},$$

$$a = 0.092 \pm 0.003 \ \text{MeV},$$

$$b = 0.063 \pm 0.006 \ \text{MeV}.$$

The shell model binding energies calculated with these values are listed in the third column of Table IV. The rms deviation between theory and experiment is 227 keV. These results deserve some comments.

The rms deviation we have attained satisfies our expectations; we are able to describe consistently at the same level of accuracy excitation energies and, valence space, ground state energies.

The value $e_v = -8.67$ MeV is close enough to the $A = 41$ value -8.36 MeV as to be considered satisfactory.

The values of the a and b parameters are small and indeed smaller than the monopole modifications of some terms of the original Kuo-Brown interaction that led to KB3 (about 300 keV).

The shell model binding energies for those nuclei not included in the fit can be compared with the extrapolated values in [19]. The differences are somewhat larger than for the measured values, without exceeding 500 keV in any case.

There are basic reasons to scale the matrix elements of the effective interactions with a term that reflects somehow the change in size of the underlying mean field. In the harmonic oscillator basis this brings in the usual $A^{1/3}$ dependence of $\hbar\omega$, which has been sometimes incorporated to sd and pf-shell effective interactions [20–22]. A more elaborate dependence has been proposed recently [23] in order to improve the description of nuclear radii. It leads to the following scaling factor:

$$\left(\frac{A_0}{A}\right)^{1/3} e^{3(A-A_0)/AA_0} \left(\frac{0.946 - 0.573\left(\frac{2T}{A_0}\right)^2}{0.946 - 0.573\left(\frac{2T}{A}\right)^2} \right)^2, \quad (6)$$

TABLE V. Shell model binding energies relative to ^{40}Ca (in MeV), compared with the experimental values (the numbers with a star are extrapolated values from [19] not included in the fit). KB3 interaction with mass dependence (see text for more details).

Nucleus	E(SM)	B_e(Theor.)	B_e(Expt.)	Δ
^{42}Ca	−2.71	19.83	19.84	−0.01
^{42}Sc$^{T=1}$	−2.71	12.34	12.64	−0.30
^{42}Sc$^{T=0}$	−2.35	12.21	12.02	0.19
^{42}Ti	−2.71	4.45	4.85	−0.40
^{43}Ca	−2.53	28.06	27.78	0.28
^{43}Sc	−6.62	25.07	24.77	0.30
^{43}Ti	−6.62	17.25	17.12	0.12
^{43}V	−2.53	4.59	5.05*	−0.45
^{44}Ca	−4.92	38.76	38.91	−0.14
^{44}Sc	−8.14	35.08	34.47	0.60
^{44}Ti	−13.67	33.08	33.42	−0.34
^{44}V	−8.14	19.16	18.94*	0.23
^{44}Cr	−4.92	6.94	7.84*	−0.90
^{45}Ca	−4.51	46.58	46.32	0.25
^{45}Sc	−10.72	46.05	45.80	0.25
^{45}Ti	−15.16	43.13	42.95	0.18
^{45}V	−15.16	35.05	35.04	0.01
^{45}Cr	−10.72	21.78	21.79*	−0.01
^{45}Mn	−4.51	6.13	6.71*	−0.58
^{46}Ca	−6.54	56.73	56.72	0.02
^{46}Sc	−11.35	54.97	54.56	0.41
^{46}Ti	−19.57	56.01	56.14	−0.13
^{46}V$^{T=1}$	−19.57	47.98	48.31	−0.33
^{46}V$^{T=0}$	−19.21	47.85	47.51	0.35
^{46}Cr	−19.57	39.57	39.92	−0.36
^{46}Mn	−11.35	22.09	22.04*	0.05
^{46}Fe	−6.54	7.41	8.13*	−0.73
^{47}Ca	−5.90	64.12	63.99	0.13
^{47}Sc	−13.58	65.39	65.20	0.19
^{47}Ti	−20.36	65.16	65.02	0.14
^{47}V	−24.20	61.38	61.31	0.07
^{47}Cr	−24.20	53.03	53.08	−0.05
^{47}Mn	−20.36	40.10	40.00*	0.10
^{47}Fe	−13.58	23.64	23.58*	0.05
^{48}Ca	−7.58	73.74	73.94	−0.20
^{48}Sc	−13.59	73.50	73.43	0.07
^{48}Ti	−23.60	76.66	76.65	0.02
^{48}V	−26.49	72.10	71.85	0.25
^{48}Cr	−31.61	69.16	69.41	−0.25
^{48}Mn	−26.49	55.14	54.81*	0.33
^{48}Fe	−23.60	42.74	43.14*	−0.40
^{48}Co	−13.59	22.61	22.61*	0.00
^{49}Sc	−15.48	83.41	83.57	−0.16
^{49}Ti	−23.70	84.95	84.79	0.16
^{49}V	−29.61	83.56	83.40	0.16
^{49}Cr	−33.96	80.02	79.99	0.03
^{49}Mn	−33.96	71.41	71.49	−0.08
^{49}Fe	−29.61	57.73	57.68*	0.05
^{49}Co	−23.70	41.89	41.90*	0.00
^{50}Ti	−26.34	95.66	95.73	−0.07
^{50}V	−30.57	92.76	92.74	0.02
^{50}Cr	−38.47	92.94	92.99	−0.05
^{50}Mn$^{T=1}$	−38.47	84.39	84.58	−0.19
^{50}Mn$^{T=0}$	−38.25	84.39	84.35	0.04
^{50}Fe	−38.47	75.46	75.64	−0.18
^{50}Co	−30.57	57.80	57.59*	0.22
^{50}Ni	−26.34	43.23	43.40*	−0.17
^{51}V	−33.37	103.71	103.79	−0.07
^{51}Cr	−39.49	102.27	102.25	0.02
^{51}Mn	−43.60	98.22	98.26	−0.04
^{51}Fe	−43.60	89.35	89.46	−0.11
^{51}Co	−39.49	75.68	75.74*	−0.06
^{51}Ni	−33.37	59.38	59.12*	0.27
^{52}Cr	−43.21	114.21	114.29	−0.08
^{52}Fe	−50.95	105.38	105.64	−0.27
^{52}Ni	−43.21	78.24	78.41*	−0.16
^{54}Fe	−58.46	129.70	129.71	−0.01
^{54}Co	−58.46	120.63	120.68	−0.05
^{54}Ni	−58.46	111.21	111.10	0.11
^{56}Ni	−72.31	142.38	141.94	0.44

where A_0 is the mass at which the effective interaction has been computed and A and T are the mass and the isospin of the nucleus with which we are dealing.

It is worth noticing that the lower pf-shell might be special when it comes to scaling, because the radii of ^{40}Ca and ^{58}Ni can be reproduced without any change in the harmonic oscillator size parameter as well as the Coulomb displacement energies [24]. On the other hand we wondered whether or not the extra global monopole correction that comes out of our fit is an artifact due precisely to the absence of mass dependence in the matrix elements. In order to settle this point we have repeated all the binding energy calculations with matrix elements scaled as in Eq. (6) with $A_0=42$ (see Table V). Afterwords, we follow exactly the same steps discussed above; we add the same Coulomb energies and proceed to fit the coefficients of the global monopole formula (4), but now with the a and b parameters scaling as the matrix elements. The values of the parameters at $A=42$ are

$$e_v=-8.61\pm0.01 \text{ MeV},$$

$$a=0.041\pm0.003 \text{ MeV},$$

$$b=0.119\pm0.006 \text{ MeV}.$$

The resulting binding energies are compared in Table V with the experimental data. The rms deviation is now 215 keV. Therefore we are led to conclude that the average quality of the agreement is insensitive to the inclusion of a mass dependence in the two-body matrix elements. Notice that the value of e_v is essentially the same as that obtained without mass dependence. On the other hand the a and b parameters are quite different from the ones obtained earlier, even if they are in the same range of values. It appears that one half of the global isoscalar monopole correction can be absorbed into the mass dependence, while the isovector correction doubles. The predictions for the binding energies not included in the fit differ from those of the previous calculation typically by 150 keV, in the direction of increasing the dis-

crepancy with the extrapolated values. Nevertheless none of these elements is decisive in making a choice between the two approaches. On the one side, Occam's razor favors the mass independent choice, on the other side, if we want to go beyond ^{56}Ni we should surely need to incorporate the mass dependence.

V. CONCLUSIONS

The new shell model code NATHAN has been used to calculate the binding energies, $M1$, $E2$, and GT sum rules of several nuclei of the pf-shell, in the full valence space, using the effective interaction KB3. These results have been used to benchmark the SMMC calculations, which we find to be in reasonable agreement with the exact results. We have also computed the binding energy of nearly all $1f_{7/2}$ nuclei, reaching the same level of agreement that we had for the excitation energies and making predictions for a number of still unavailable masses. We also show that the inclusion of a mass dependence in the two-body matrix elements is not critical for the description of the binding energies in this region.

ACKNOWLEDGMENTS

This work was partially supported by the IN2P3-France, CICYT-Spain agreements, and by a DGES (Spain) grant PB96-053.

[1] E. Caurier, A.P. Zuker, A. Poves, and G. Martínez-Pinedo, Phys. Rev. C **50**, 225 (1994).
[2] E. Caurier, J.L. Egido, G. Martínez-Pinedo, A. Poves, J. Retamosa, L.M. Robledo, and A.P. Zuker, Phys. Rev. Lett. **75**, 2466 (1995).
[3] G. Martínez-Pinedo, A.P. Zuker, A. Poves, and E. Caurier, Phys. Rev. C **55**, 187 (1997).
[4] T.T.S. Kuo and G.E. Brown, Nucl. Phys. **A114**, 241 (1968).
[5] A. Poves and A.P. Zuker, Phys. Rep. **70**, 235 (1980).
[6] E. Caurier, computer code ANTOINE, CRN, Strasbourg (1989).
[7] C. Ur *et al.*, Phys. Rev. C **58**, 3163 (1998).
[8] F. Nowacki and E. Caurier, coupled code NATHAN, CRN, Strasbourg (1995).
[9] F. Nowacki, Ph.D. thesis, Strasbourg, 1996.
[10] S.E. Koonin, D.J. Dean, and K. Langanke, Phys. Rep. **278**, 1 (1997).
[11] M. Honma, T. Mizusaki, and T. Otsuka, Phys. Rev. Lett. **77**, 3315 (1996).
[12] R.R. Whitehead, A. Watt, B.J. Cole, and I. Morrison, Adv. Nucl. Phys. **9**, 123 (1977).
[13] J.B. French, E.C. Halbert, J.B. McGrory, and S.S.M. Wong, Adv. Nucl. Phys. **3**, 237 (1969).
[14] K. Langanke, D.J. Dean, P.B. Radha, Y. Alhassid, and S.E. Koonin, Phys. Rev. C **52**, 718 (1995).
[15] Y. Alhassid, D.J. Dean, S.E. Koonin, G. Lang, and W.E. Ormand, Phys. Rev. Lett. **72**, 613 (1994).
[16] M.S. Anthony, J. Britz, J.B. Bueb, and A. Pape, At. Data Nucl. Data Tables **33**, 448 (1985).
[17] M.S. Anthony, J. Britz, and A. Pape, At. Data Nucl. Data Tables **40**, 10 (1988).
[18] J. Duflo and A. Zuker, Phys. Rev. C **52**, R23 (1995).
[19] G. Audi and A.H. Wapstra, Nucl. Phys. **A595**, 409 (1995).
[20] B.H. Wildenthal, Prog. Part. Nucl. Phys. **11**, 5 (1984).
[21] W.A. Richter, M.G. Van der Merwe, R.E. Julies, and B.A. Brown, Nucl. Phys. **A523**, 325 (1991).
[22] J. Retamosa, E. Caurier, F. Nowacki, and A. Poves, Phys. Rev. C **55**, 1255 (1997).
[23] J. Duflo and A. Zuker (private communication).
[24] J.M. Gomez, Phys. Lett. **62B**, 25 (1976).